Suppression of projectile-electron excitations in collisions with a free-electron gas of metals

C. C. Montanari,[1,2] J. E. Miraglia,[1,2] and N. R. Arista[3]
[1]*Instituto de Astronomía y Física del Espacio, Consejo Nacional de Investigaciones Científicas y Tecnológicas, Casilla de Correo 67, Sucursal 28, 1428 Buenos Aires, Argentina*
[2]*Departamento de Física, FCEyN, Universidad de Buenos Aires, Buenos Aires, Argentina*
[3]*Instituto Balseiro, Centro Atómico Bariloche, 8400 Bariloche, Argentina*
(Received 19 April 2000; published 18 October 2000)

Excitation and ionization of hydrogenic projectiles in collisions with metal free-electron gas are analyzed in the high but nonrelativistic energy regime. Transition matrix elements are calculated in the first Born approximation, and the free-electron gas response is described by using the Mermin-Lindhard dielectric function. Projectile excitation and loss probabilities per unit length are found to be smaller than those corresponding to the collisions with a wave packet of single electrons of equivalent density. This behavior is explained in terms of the collective effect (shielding) of the free-electron gas and depends on the energy transferred to the atomic electron and on the impact velocity. By comparing results obtained using a binary collisional formalism and those using the dielectric formalism, we estimate the plasmon excitation contribution to the total probabilities.

PACS number(s): 34.50.Dy, 34.50.Bw

I. INTRODUCTION

The interaction of fast ions and other charged particles with matter has been widely analyzed [1–7]. Stopping power [8–10], charged-state fractions [11–14], x-ray emission [15–17], and electron emission [18,19] constitute powerful techniques for material analysis. Realistic models of this phenomenon must incorporate the description of the interaction between the projectile and the whole solid, that is, the screened nuclei, the core electrons, and the free-electron gas (FEG), in the case of metallic solids. In the present work we restrict our analysis to the interaction of the projectile with the FEG.

Traditionally two different approaches have been used to describe this interaction in the intermediate and high velocity regimes:

i) The dielectric formalism (DF), in which the target electrons are considered to respond to the passage of the projectile inducing a wake potential [7,8,17–19]. The wake follows the motion of the projectile with the same velocity so that it remains as a stationary perturbation of the medium as seen from the projectile. This approach gives an account of the two basic modes of energy and momentum absorption by the electrons of the FEG [8], namely, single-particle excitations (or electron-hole pair excitations), and *collective* or plasmon excitations.

ii) The binary collisional (BC) formalism, in which the projectile is subject to a series of binary collisions with the *individual* electrons of the FEG [10,13–16]

Recent articles [10,16] have pointed out the dichotomy between the physical pictures represented by DF and BC descriptions. In this contribution we present a link between both formalisms [10] in dealing with hydrogenic projectiles interacting with metal solids. We are interested in electron excitation, de-excitation, and loss due to the interaction with the FEG. It is also a purpose of the present work to investigate the contribution of the collective effects (plasmons and shielding) to the total transition probabilities per unit length. These in-solid probabilities are compared with those obtained in out-solid experiments of electron-atom excitation and ionization.

The present theory makes use of the first Born approximation for the calculation of the atomic form factors [20,21], and a wake potential to express the collective response of the FEG to an external perturbation. The Mermin-Lindhard dielectric function [22] is used. The shifting of the binding energies of the moving projectile embedded in the FEG is accounted for within the spherical approximation.

The work is organized as follows. In Sec. II the theoretical model is presented. This includes the description of the dielectric formalism (Sec. II A) and the binary formalism (Sec. II B) for excitation and electron loss of the projectile electron due to the interaction with the FEG; the development of a model for the binding energies of a moving projectile within the FEG (Sec. II C); and the comparison between excitation and electron loss probabilities per unit length in atom-FEG (in-solid) and atom-electron (out-solid) collisions (Sec. II D). In Sec. III we present the results of probabilities per unit length and energy spectrum for different hydrogenic projectiles such as H, He^+, Li^{2+}, and B^{4+} colliding with aluminum FEG. The impact velocities considered here are $v \geqslant Z_P, v_F$ (with v_F being the Fermi velocity of the FEG). Finally, the conclusions are summarized in Sec. IV. Atomic units are used unless otherwise stated.

II. THEORY

A. Dielectric formalism

Let us consider a projectile composed of a heavy nucleus of charge Z_P and an active electron, moving with velocity v inside a solid. Due to the interaction of the projectile with the whole FEG, the bound electron can suffer transitions to excited states of the ion, or even be ionized. This colliding system can be schematically represented by the process

$$(P^{Z_P+}+e^-)_{i,\vec{K}_i}+\mathrm{FEG} \rightarrow (P^{Z_P+}+e^-)_{f,\vec{K}_f}+\mathrm{FEG}^*, \quad (1)$$

where $i(f)$ is the initial (final, either bound or continuum) atomic state, $\vec{K}_i(\vec{K}_f)$ is the incident (final) momentum of the projectile in the laboratory reference frame, and FEG* denotes an excited state of the FEG, either collective or of single electrons.

According to the dielectric formalism [7,18], the probability of transition per unit length for the reaction (1) is

$$W_{DF}=-\frac{1}{\pi^2 v}\int_0^\infty d\omega \int \frac{d\vec{q}}{q^2}|F_{if}(\vec{q})|^2 \times \mathrm{Im}\left[\frac{1}{\epsilon(q,\omega,\gamma)}\right]\delta(\vec{v}\cdot\vec{q}-\Delta\varepsilon-\omega), \tag{2}$$

where ω and $\vec{q}$ are the energy and momentum gained by the FEG either in plasmon or single-electron excitations, $\Delta\varepsilon$ is the change of energy of the projectile electron, $\epsilon(q,\omega,\gamma)$ is the dielectric function [4], and γ is the damping rate of the plasmons so that the lifetime is $\tau=1/\gamma$ [8]. The atomic form factor $F_{if}\ (\vec{q})$ is [23]

$$F_{if}(\vec{q})=\int \varphi_f^*(\vec{r})e^{i\vec{q}\cdot\vec{r}}\varphi_i(\vec{r})d\vec{r}, \tag{3}$$

with $\varphi_i(\vec{r})$ and $\varphi_f(\vec{r})$ the initial and final unperturbed wave functions of the hydrogenic projectile, respectively. The energy conservation

$$\omega=\vec{v}\cdot\vec{q}-\Delta\varepsilon, \tag{4}$$

is included in Eq. (2) through the delta function. Terms of the order of $q^2/2\nu_P$, where ν_P is the projectile atomic mass, are neglected in Eq. (4) since $\nu_P\gg 1$. Equation (2) can be expressed as

$$W_{DF}=-\frac{2}{\pi v^2}\int_{\Delta\varepsilon/v}^\infty \frac{dq}{q}\int_0^{qv-\Delta\varepsilon} d\omega \times |F_{if}(q,\omega)|^2\,\mathrm{Im}\left[\frac{1}{\epsilon(q,\omega,\gamma)}\right], \tag{5}$$

where a simple change of variables has been performed by using the energy conservation expressed in Eq. (4). The transition probability per unit length W_{DF} involves both modes of absorption of energy and momentum by the FEG, single-particle excitations (binary collisions) and plasmon excitations (collective modes) [2,8]. For this reason W_{DF} will also be referred to hereafter as *total* transition probability. In the next subsection we develop a formalism to calculate transition probabilities by considering only the binary collisions of the projectile with the single electrons of the FEG [10], and compare both results.

B. Binary collisional formalism

If we consider the scattering of the *individual* electrons of the FEG, the colliding system can be schematically represented by the tree-particle process,

$$(P^{Z_P+}+e^-)_{i,\vec{K}_i}+e^-_{\vec{k}_i}\rightarrow(P^{Z_P+}+e^-)_{f,\vec{K}_f}+e^-_{\vec{k}_f}. \tag{6}$$

As in Eq. (1), the final atomic state f can be either bound or continuum. The energy gained by the single electron is defined as

$$\omega=k_f^2/2-k_i^2/2=\frac{p^2}{2}-\vec{p}\cdot\vec{k}_i, \tag{7}$$

where $\vec{p}=\vec{k}_i-\vec{k}_f$ is the momentum transferred and $\vec{k}_i(\vec{k}_f)$ is the electronic initial (final) momentum in the laboratory reference frame. The energy conservation can be expressed as

$$\omega=\vec{v}\cdot\vec{P}-\Delta\varepsilon, \tag{8}$$

with $\vec{P}=\vec{K}_i-\vec{K}_f$, the transferred momentum of the projectile. Again, terms of the order of $P^2/2\nu_P$ are neglected. Note that the linear momentum conservation implies $\vec{P}=-\vec{p}$; i.e., the momentum *lost* by the projectile equals the momentum *absorbed* by the electron of the FEG, as will be observed in Eq. (10) below.

1. Excitation

The Fermi Golden Rule states that the differential probability per unit length W_{BC} for the process represented by Eq. (6) is given by

$$\frac{dW_{BC}}{d\vec{k}_i\,d\vec{P}d\vec{p}}=\frac{2\pi}{v}\delta\left(\omega-\frac{p^2}{2}+\vec{p}\cdot\vec{k}_i\right)|T_{if}|^2 \times 2\Theta(K_F-k_i)\Theta(k_f-K_F), \tag{9}$$

where $T_{if}=\langle\varphi_f|V|\Psi_i^+\rangle$ is the transition matrix element, $V=V_{Pe}+V_{ee}$ is the perturbative potential between the projectile nucleus and FEG electron (V_{Pe}), and between the projectile electron and the FEG electron (V_{ee}). The step function $2\Theta(K_F-k_i)$ describes the Fermi distribution at $T=0$ °K, and $\Theta(k_f-K_F)$ accounts for the Pauli exclusion principle.

The transition matrix element in first Born approximation is

$$T_{if}^B=\frac{1}{(2\pi)^{3/2}}\delta(\vec{p}+\vec{P})[\tilde{V}_{Pe}(\vec{P})F_{if}(\vec{P}/\nu_P)+\tilde{V}_{ee}(\vec{P})F_{if}(\vec{P})], \tag{10}$$

where $\tilde{V}_{Pe}(\vec{P})$ and $\tilde{V}_{ee}(\vec{P})$ are the Fourier transforms of the perturbative potential, and $\delta(\vec{p}+\vec{P})$ guarantees the linear momentum conservation mentioned before. The first term in Eq. (10) corresponds to the interaction between the electron of the FEG and the projectile nucleus. As $\nu_P\gg 1$, this term remains essential in the elastic channel, but negligible in the inelastic ones due to the orthogonality of the wave functions. It means that the main contribution to the transition matrix element comes from the electron-electron interaction.

We propose a wake potential whose Fourier transform reads

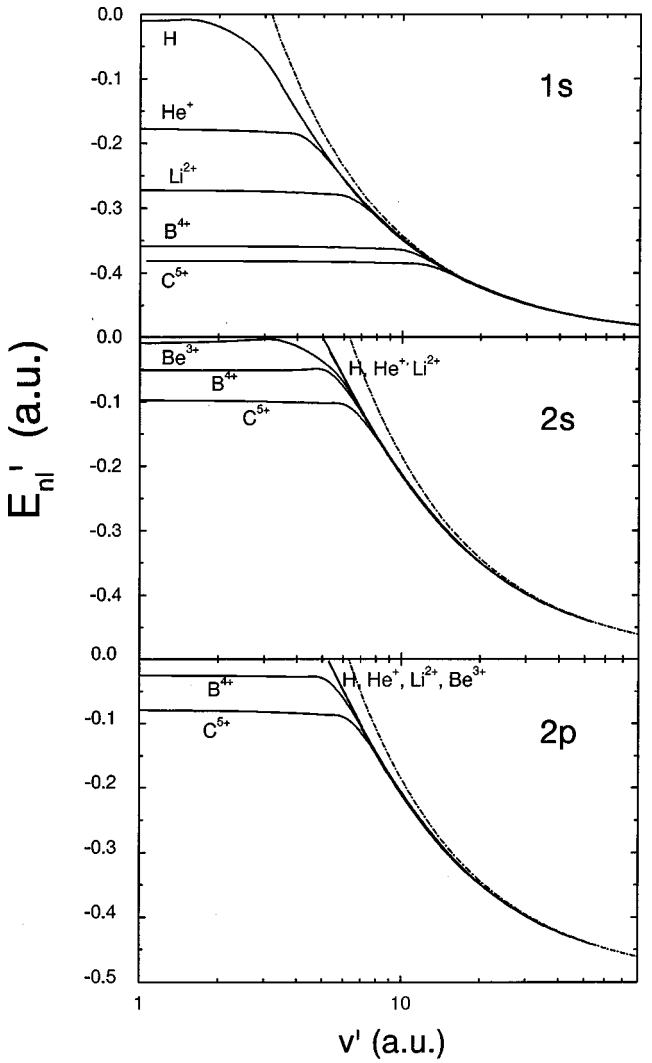

FIG. 1. Scaling binding energies E'_{nl} of a moving projectile inside the solid FEG, plotted as a function of the scaled velocity v' given by Eq. (25). Solid line, our results for different hydrogenic projectiles inside aluminum FEG; dash-dot line, universal expression of Müller and Burgdörfer [27]. The different projectiles and bound states are displayed in the figure.

$$\tilde{V}_{ee}(\vec{P}) = \sqrt{\frac{2}{\pi}} \frac{1}{P^2 \epsilon(P,\omega,\gamma)}. \tag{11}$$

The integration of Eq. (9) on $\vec{k}_i$ has a closed solution that can be expressed in terms of the Lindhard dielectric function in the following way [1,6]:

$$\int d\vec{k}_i \Theta(K_F - k_i)\Theta(k_f - K_F)\,\delta(\omega - p^2/2 + \vec{p}\cdot\vec{k}_i) = \pi p^2 \,\mathrm{Im}\,\epsilon_L(p,\omega,0^+)\Theta(\omega), \tag{12}$$

where $\epsilon_L(p,\omega,0^+)$ is the Lindhard dielectric function [1] in the limit $\gamma \to 0^+$.

For historical reasons, it is convenient to use $\vec{q} = -\vec{p}$, the momentum absorbed by the electron of the FEG, so that $\vec{q} = \vec{P}$. Using these results, the differential probability per unit length of Eq. (9) integrated on $\vec{p}$ and $\vec{k}_i$ reads

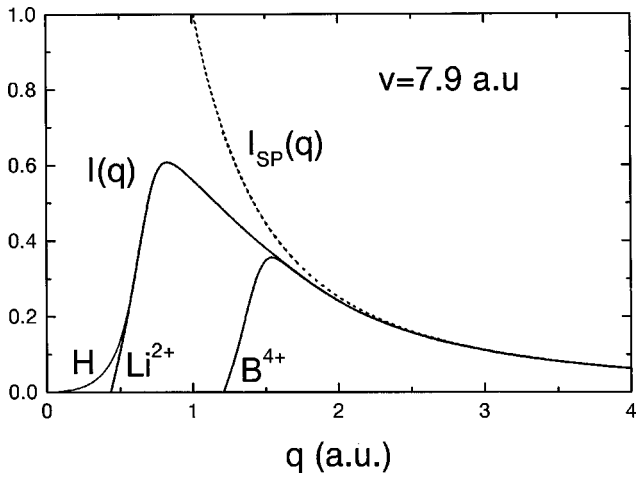

FIG. 2. Function $I(q)$ given by Eq. (31) for excitation to the $n=2$ state of different hydrogenic projectiles colliding with aluminum FEG, at impact velocity $v=7.9$ a.u. The result of $I(q)$ obtained with the Mermin-Lindhard dielectric function [22] is plotted together with the single-particle approximation given by Eq. (32).

$$\frac{dW_{BC}}{d\vec{q}} = \frac{1}{\pi^2 v q^2} |F_{if}(\vec{q})|^2 \frac{\mathrm{Im}\,\epsilon_L(q,\omega,0^+)}{|\epsilon(q,\omega,\gamma)|^2} \Theta(\omega). \tag{13}$$

The energy spectrum is defined as the differential probability per unit length and per unit of energy gained by the FEG, $P(\omega) = dW/d\omega$. For electron projectile excitation by binary collisions with the single electrons of the FEG we obtain

$$P_{BC}(\omega) = -\frac{2}{\pi v^2} \int_{(\Delta\varepsilon+\omega)/v}^{\infty} \frac{dq}{q} |F_{if}(q,\omega)|^2 \times \mathrm{Im}\left[\frac{1}{\epsilon(q,\omega,\gamma)}\right] U_\epsilon(q,\omega,\gamma), \tag{14}$$

where $U_\epsilon(q,\omega,\gamma) = \mathrm{Im}\,\epsilon_L(q,\omega,0^+)/\mathrm{Im}\,\epsilon(q,\omega,\gamma)$. The form factor $F_{if}(\vec{q})$ has been expressed in terms of q and ω by using Eq. (8) and making a simple change of variables $d\vec{q} \to q dq\ d\omega/v d\varphi$. The azimuthal symmetry of the problem has already been taken into account in Eq. (14).

The total probability per unit length is then

$$W_{BC} = \int_0^\infty P_{BC}(\omega) d\omega = -\frac{2}{\pi v^2} \int_{\Delta\varepsilon/v}^{\infty} \frac{dq}{q} \int_0^{qv-\Delta\varepsilon} d\omega \times |F_{if}(q,\omega)|^2 \mathrm{Im}\left[\frac{1}{\epsilon(q,\omega,\gamma)}\right] U_\epsilon(q,\omega,\gamma), \tag{15}$$

where we exchange the order of the integrals on q and ω to compare W_{BC} with the dielectric formalism result W_{DF} given by Eq. (5). The equality between Eq. (5) and Eq. (15) would require $U_\epsilon(q,\omega)=1$ in all the range of q and ω. This is never satisfied, even in the limit of small γ [10], where

$$U_\epsilon(q,\omega,\gamma)\rightarrow_{\gamma\rightarrow 0^+}\begin{cases} 0 & \text{if} \quad (\omega-q^2/2)^2\geqslant q^2K_F^2 \\ 1 & \text{if} \quad (\omega-q^2/2)^2<q^2K_F^2, \end{cases} \tag{16}$$

in agreement with the energy conservation in a binary collision. In the dielectric formalism this restriction disappears, taking into account not only the single-electron excitations but the collective absorption of energy and momentum, too [2,8]. Thus, the difference between Eq. (5) and Eq. (15) lead us to isolate the plasmon excitation contribution to the total probability per unit length.

Together with the excitation of the projectile electron, $\Delta\varepsilon>0$, we analyze the de-excitation processes, $\Delta\varepsilon<0$. The energy spectrum can be generalized for these processes by changing in Eq. (14) the lowest limit of the integral from $(\Delta\varepsilon+\omega)/v$ to $|\Delta\varepsilon+\omega|/v$. We find that the de-excitation energy spectrum verifies

$$P_{fi}(\omega)=-P_{if}(-\omega). \tag{17}$$

Here $P_{if}(\omega)$ represents either P_{BC} or P_{DF} for the projectile electron transition $i\rightarrow f$. The difference in sign is due to the parity of the imaginary part of the Lindhard dielectric function [1].

2. Electron loss

In projectile electron loss processes, the final state in Eq. (6) is $f\equiv\vec{k}$, with $\vec{k}$ being the electron momentum relative to the ion. This process is equivalent to the Auger electron loss process analyzed by Rösler *et al.* [18]. The Fermi Golden Rule for the differential probability per unit length and per unit of $\vec{k}$, is obtained by replacing W_{BC} with $dW_{BC}/d\vec{k}$ in Eq. (9). The ionization transition matrix elements are calculated in the first Born approximation in the usual way [21,24]. The atomic form factors $F_{i\vec{k}}(q,\omega)$ are expanded in terms of the angular momentum, considering in our calculations a maximum angular momentum $L_{\max}=6$. Analogously to excitation, the electron loss probability per unit length W_{BC} reads

$$W_{BC}=-\frac{2}{\pi v^2}\int d\vec{k}\Theta(|\overline{k}+\overline{v}|-K_F)\int_{\Delta\varepsilon/v}^{\infty}\frac{dq}{q}\int_0^{qv-\Delta\varepsilon}d\omega \times|F_{i\vec{k}}(q,\omega)|^2\,\mathrm{Im}\left[\frac{1}{\epsilon(q,\omega,\gamma)}\right]U_\epsilon(q,\omega,\gamma), \tag{18}$$

and the energy spectrum is

$$P_{BC}(\omega)=\frac{dW_{BC}}{d\omega} =-\frac{2}{\pi v^2}\int d\vec{k}\Theta(|\overline{k}+\overline{v}|-K_F) \times\int_{(\Delta\varepsilon+\omega)/v}^{\infty}\frac{dq}{q}|F_{i\vec{k}}(q,\omega)|^2\,\mathrm{Im}\left[\frac{1}{\epsilon(q,\omega,\gamma)}\right] \times U_\epsilon(q,\omega,\gamma). \tag{19}$$

By comparing these expressions with Eq. (1) of Rösler *et al.* [18], the probability per unit length and energy spectrum in the dielectric formalism, W_{DF} and $P_{DF}(\omega)$, respectively, are obtained from Eqs. (18) and (19) by replacing $U_\epsilon(q,\omega,\gamma)=1$ [10].

C. Binding energies of a moving projectile inside the solid

When the projectile penetrates the FEG, the electrons react collectively leading to a dynamical screening of the ion. As a consequence of this, the binding energies are relaxed depending on the ion velocity, no longer being $-Z_P^2/2n^2$, as in the isolated hydrogenic atom spectrum. The aim of this subsection is to estimate the binding energies E_{nl} of a moving ion embedded in a FEG within the spherical approximation. The Hamiltonian of the system is $[-1/2\nabla_r^2+V(r)-E_{nl}]\psi_{nl}=0$, where $V(r)$ is the induced potential giving the response of the medium to the perturbation created by a heavy ion moving within a FEG,

$$V(\vec{r})=\frac{1}{(2\pi)^{3/2}}\int d\vec{q}\frac{\widetilde{V}_C(q)}{\epsilon(q,u,\gamma)}\exp(i\vec{q}\cdot\vec{r}), \tag{20}$$

with $u=\vec{v}\cdot\vec{q}$ and v the ion velocity. The Fourier transform of the Coulomb potential $\widetilde{V}_C(q)$ in Eq. (20) is

$$\widetilde{V}_C(q)=-\sqrt{\frac{2}{\pi}}\frac{Z_P}{q^2}. \tag{21}$$

The Legendre angular expansion of the induced potential given by Eq. (20) reads

$$V(\vec{r})=\sum_{L=0}^{\infty}V_L(r)P_L(\cos\theta), \tag{22}$$

with $cos\ \theta=\hat{v}\cdot\hat{r}$. The terms $V_L(r)$ are obtained by expanding the plane wave $\exp(i\vec{q}\cdot\vec{r})$ and the inverse of the dielectric function in Legendre polynomials,

$$V_L(r)=-\frac{Z_P}{\pi v}(2L+1)i^L\int_0^{\infty}\frac{dq}{q}j_L(qr)\int_0^{qv}du\,P_L\left(\frac{u}{qv}\right) \times\left[\frac{1}{\epsilon(q,u,\gamma)}+\frac{(-1)^L}{\epsilon^*(q,u,\gamma)}\right], \tag{23}$$

TABLE I. Classically scaled cross sections σZ^4 for electron impact excitation of H($1s$), and electron impact ionization of $He^+(1s)$. The final state is indicated explicitly in the table, with k being the symbol for the continuum final state. Notation: 1B, present results in the first Born approximation; a, experimental measurements of Kauppila *et al.* [30] modified by van Wyngaarden *et al.* [35]; b, values calculated from the experimental results of Long *et al.* [33], and Ott [34]; c, experimental ionization cross sections of Shah *et al.* [31] and Peart *et al.* [32]. Atomic units are used.

v/Z	σZ^4	1B	Experiments	Ref.
2.71	$2s$	0.18	0.12 ± 0.01	a
	$2p$	2.4	1.95 ± 0.09	b
	k	2.9	2.2	c
3.83	$2s$	0.093	0.079 ± 0.009	a
	$2p$	1.5	1.41 ± 0.06	b
	k	1.6	1.5	c
5.07	$2s$	0.054	0.044 ± 0.006	a
	k	1.0	0.96	c

where $j_L(qr)$ are the spherical Bessel functions [21]. For $L=0$, the spherical potential reduces to

$$V_0(r)=-\frac{2Z_P}{\pi v}\int_0^\infty dq\,\frac{\sin qr}{q^2 r}\int_0^{qv} du\,\mathrm{Re}\left[\frac{1}{\epsilon(q,u,\gamma)}\right]. \tag{24}$$

In general, for L odd (even), the integrand involves the imaginary (real) part of the inverse of the dielectric function. The binding energies E_{nl} of one electron in the central potential $V_0(r)$ are calculated using the code of Salvat *et al.* [25] for different projectile charges and velocities inside aluminum FEG.

In order to plot the results in a comprehensive way, we use the Coulomb scaling for the energies and the dynamic screening approximation [7] for the velocities,

$$E'_{nl}=E_{nl}\frac{n^2}{Z_P^2},\quad v'=v\frac{Z_P}{n\omega_p}, \tag{25}$$

with ω_p being the plasmon frequency. In Fig. 1 we plot E'_{nl} as a function of v' for the atomic states $1s$, $2s$, and $2p$. It is remarkable that the $1s$ state of hydrogen survives even at low velocities ($v<1$). The small binding energies of H at low velocities are consistent with the results of Rogers *et al.* [26]. For the $n=2$ bound states inside the solid, the threshold velocities obtained are $v=6$ for H, and $v=3$ for He^+. For higher projectile nuclear charges, the $n=2$ bound states are possible at velocities even lower than these. As can be observed in Fig. 1, for large velocities, the results for different hydrogenic projectiles follow a trend closing on a universal form. Also displayed in Fig. 1 is the universal expression for the eigenenergies of the electronic bound states of fast charged particles in solids posed by Müller and Burgdörfer, [27]

TABLE II. Minimum velocity for plasmon excitation given by Eq. (37) for the collisions of different atomic projectiles with aluminum FEG ($\omega=0.566$). Atomic units are used.

	H	He^+	Li^{2+}	B^{4+}
$v_{1s\to n=2}$	1.2	2.9	6.1	16
$v_{1s\to continuum}$	1.2	3.6	7.8	21

$$E'^{B}_{nl}=-\frac{1}{2}+\frac{\pi n}{2v'}+\frac{\pi^2 sn}{2v'^2}, \tag{26}$$

with s being the electric quantum number. These authors [27] derived Eq. (26) by diagonalizing an axially symmetric induced potential in the plasmon pole approximation. We use $s=0$ to obtain the values shown in Fig. 1 because we employ a spherical potential. It can be observed that Eq. (26) follows the universal tendency at high velocities, but differs from our curves as the velocity decreases.

Along this article we use the orbital effective charge of a moving atom inside a solid as given by

$$Z_{nl}=\sqrt{-2n^2E_{nl}}. \tag{27}$$

The binding energies E_{nl} so obtained are just a first-order calculation. A second order can be obtained by including in Eq. (21) the electron density of the bound state. Important corrections are expected for the smallest projectile charges.

D. Link between atom-FEG and atom-electron collisions

In this subsection we make a simple link between atom-FEG (in-solid) and atom-electron (out-solid) collisions by approximating the atom-FEG probabilities per unit length using the single-particle dielectric function, $\epsilon\simeq\epsilon_{SP}$ [2,7,28]. In the limit $\gamma\to0^+$ (no plasmon dispersion) and $q^2\gg2\omega_p$, the single-particle approximation satisfies

$$\mathrm{Im}\left[\frac{1}{\epsilon_{SP}(q,\omega,\gamma)}\right]=-\pi\frac{\omega_p^2}{q^2}\;\delta(\omega-q^2/2). \tag{28}$$

The excitation probability per unit length using this approximation reduces to

$$W_{SP}=\frac{2\omega_p^2}{v^2}\int_{\Delta\varepsilon/v}^\infty\frac{dq}{q^3}|F_{if}(q,\omega=q^2/2)|^2. \tag{29}$$

The form factor is evaluated in $\omega=\vec{v}\cdot\vec{q}-\Delta\varepsilon=q^2/2$, which is the expression for the energy conservation in the collision of an atom and an electron moving with relative velocity $\vec{v}$, and momentum transferred to the electron $\vec{q}$. Then Eq. (29) can be expressed as

$$W_{SP}=n_e\sigma^{gas}, \tag{30}$$

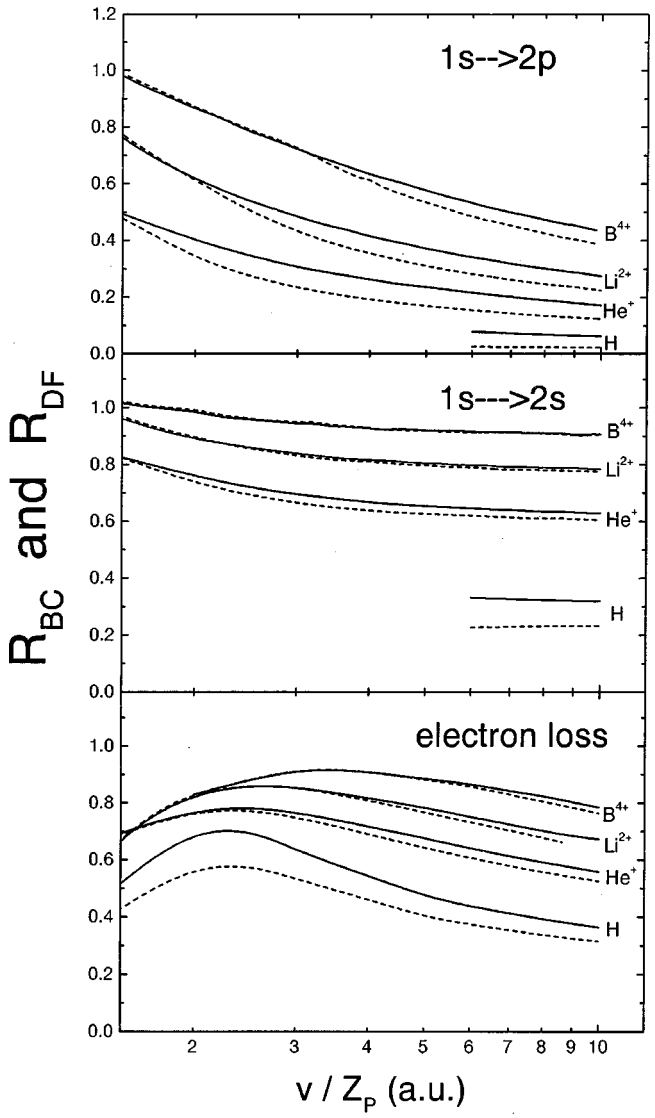

FIG. 3. Ratio of in-solid to out-solid probabilities per unit length for different hydrogenic projectiles in collisions with aluminum FEG. The different projectiles and transitions considered here are pointed out in the figure. Notation: solid lines, dielectric formalism curves R_{DF}, given by Eq. (36); dashed lines, the binary collisional results R_{BC}, given by Eq. (35).

where $n_e=\omega_p^2/4\pi$ is the electronic density and σ^{gas} is the known high velocity limit for the atom-electron cross sections in the first Born approximation [20,23]. This relation for large transferred momentum is consistent with that found by Ritchie [2] 40 years ago.

To inspect this approximation we define the function

$$I(q)=\int_0^{qv-\Delta\varepsilon} d\omega\,\mathrm{Im}\left[\frac{-1}{\epsilon(q,\omega,\gamma)}\right], \tag{31}$$

as introduced by Glick and Ferrell [28]. In the single-particle approximation expressed by Eq. (28), Eq. (31) reduces to

$$I_{SP}(q)=\pi\omega_p^2/q^2. \tag{32}$$

Note that when the atomic form factor depends only on q, and not on ω (the angular part of $\vec{q}$), i.e., for the atomic excitations $1s\rightarrow 2s$ or $1s\rightarrow 2p$, the probability per unit length given by Eq. (15) reads

$$W_{BC}=-\frac{2}{\pi v^2}\int_{\Delta\varepsilon/v}^{\infty}\frac{dq}{q}|F_{if}(q)|^2 I(q). \tag{33}$$

The energy integral $I(q)$ encloses the whole dependence of the probability per unit length on the collective response of the medium. In Fig. 2 we plot $I(q)$ and $I_{SP}(q)$, given by Eqs. (31) and (32) respectively, for different projectiles interacting with the FEG at $v=7.9$ a.u. This velocity corresponds to the experimental measurements of Tinschert *et al.* [29] for ionization of Li^{2+} by 850 eV electron impact. The dielectric function used to evaluate $I(q)$ is the Mermin-Lindhard one [22]. We can see in this figure that they have the same limit as q increases, but for $q\rightarrow\Delta\varepsilon/v$, Eq. (31) tends to zero while the single-particle approximation grows as $1/q^2$. The smaller $\Delta\varepsilon/v$ is, the greater the difference between $I(q)$ and $I_{SP}(q)$ will be. This analysis implies that the probabilities per unit length corresponding to atom-FEG collisions are generally *lower* than those corresponding to the collisions of the atom and an equivalent density of single electrons,

$$W_{BC}\lesssim W_{SP}=n_e\sigma_{if}^{gas}. \tag{34}$$

This suppression of the probabilities per unit length in the collision of hydrogenic projectiles with the solid FEG grows up as the minimum momentum absorbed by the FEG, $\Delta\varepsilon/v$, diminishes (either by increasing the impact velocity or decreasing the energy transferred to the atomic electron). This behavior does not depend on the approximation used to describe the collisional system, but only on the response of the medium. This link between the atom-FEG and atom-electron collisions is valid either for atomic excitation or electron loss processes.

In order to analyze this decline in the probabilities we define the ratio

$$R_{BC}=\frac{W_{BC}^{solid}}{W_{SP}}, \tag{35}$$

where $W_{BC}^{solid}=W_{BC}(Z_{nl})$ is the binary collisional probability per unit length given by Eq. (15) or (18), taking into account the orbital effective charge inside the solid as given by Eq. (27). Instead, W_{SP} is calculated from Eq. (30) by using the actual nuclear charge of the projectile to obtain atom-electron cross sections [20,21,24]. A similar ratio is defined for the probabilities per unit length in the dielectric formalism

$$R_{DF}=\frac{W_{DF}^{solid}}{W_{SP}}. \tag{36}$$

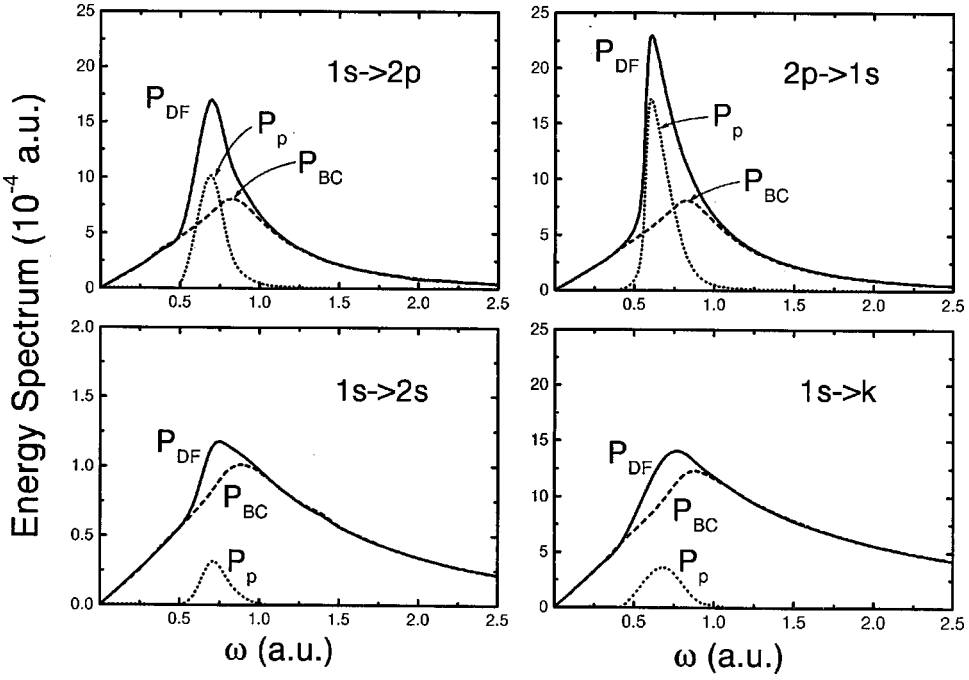

FIG. 4. Energy spectrum as a function of the energy gained by the FEG, for projectile electron excitation $1s\rightarrow 2s$, $1s\rightarrow 2p$, de-excitation $2p\rightarrow 1s$, and electron loss. The colliding system considered is $He^+ + FEG(Al)$ at impact velocity $v=6$ a.u. Notation: solid lines, dielectric formalism results P_{DF}; dashed lines, binary collisional results P_{BC}; dotted line, plasmon excitation contribution $P_p = P_{DF} - P_{BC}$.

III. RESULTS

Probabilities per unit length and energy spectrum are calculated within the first Born approximation [20,21] and employing the Mermin-Lindhard dielectric function of the medium [22]. Projectile electron excitation and loss are analyzed employing the usual dielectric formalism (Sec. II A), and the binary collisional formalism (Sec. II B).

We compare the first Born approximation employed in all these theoretical calculations, with the experimental results [29–36] for excitation and ionization of hydrogenic atoms by single-electron impact (out-solid collisions). We reproduce the known behavior of the first Born approximation in electron-atom collisions [20], i.e., it overestimates the cross sections at intermediate velocity and tends to the experimental data in the high velocity limit. In general, for the different projectiles considered, we get an overestimation of the cross sections at $v/Z=3$ of less than 25% as compared with the experimental values for excitation $1s\rightarrow 2s$ [30] and ionization [29,31,32]. For excitation $1s\rightarrow 2p$ at the same velocity, we obtain cross sections in the first Born approximation only 7 % over the experimental data [33,34]. Some experimental results are shown in Table I together with our first Born cross sections, conveniently scaled as σZ^4. The experimental excitation cross sections in this table correspond to e-H collisions [30,33–36], while the ionization values correspond to e-He^+ collisions [32].

We also compare our results for electron loss and excitation of the projectile electron due to the interaction with the FEG only, with theoretical results obtained by considering the interaction with the whole target atom [14,37]. For a He^+ projectile colliding with an aluminum solid at an impact velocity of 3.16 a.u, our electron loss and excitation $1s\rightarrow n=2$ cross sections are about 15% and 40%, respectively, those of Kaneko [37], taking into account the whole frozen target. For H^0impact the contribution is expected to be larger. The larger Z_P is, the smaller the influence of the FEG will be.

A. Probabilities per unit length

We calculate the probabilities per unit length for projectile electron excitation $1s\rightarrow 2s$ and $1s\rightarrow 2p$, and for electron loss in the collisions of H^0, He^+, Li^{2+}, and B^{4+} projectiles with the aluminum FEG ($\omega_p=0.566, \gamma=0.037$ [38]). In Fig. 3 we display the ratios R_{DF} and R_{BC} for the different colliding systems. In each case we include the results in the velocity range where the excited bound state within the FEG is possible considering the spherical approximation (see Fig. 1). Two main conclusions are derived from this figure. First, the difference between the dielectric and the collisional results reveals the contribution of plasmon excitation included only in the former. Figure 3 shows that plasmon excitation is negligible at the lower velocities considered here, giving the binary collisional formalism a good estimation of the total probability per unit length [18,19]. As the impact velocity increases, the plasmon excitation becomes more important. This feature is consistent with Fig. 2 of Rösler *et al.* [18].

The minimum velocity for a collective excitation to occur can be obtained assuming that the curve $qv-\Delta\varepsilon$ intersects the region of energy and momentum excitations in a $\omega-q$ plot, just at the cutoff momentum for the plasmon mode, $q=q_c$. Mathematically, it occurs when

$$q_c v_{\min} - \Delta\varepsilon = \frac{q_c^2}{2} + q_c v_F . \tag{37}$$

For metallic electron densities, a satisfactory estimation of q_c is given by $q_c \simeq \omega_p / v_F$ [5] ($q_c \simeq 0.622$ [38] for aluminum FEG). In the elastic channel $1s\rightarrow 1s(\Delta\varepsilon=0)$, the minimum velocity obtained from Eq. (37) is 1.2 a.u. For projectile electron transitions $1s\rightarrow n=2$ and $1s\rightarrow$continuum, the

threshold velocities for plasmon excitation are given in Table II. In obtaining these velocities, we take into account the velocity-dependent binding energies inside the solid displayed in Fig. 1. The results shown in Table II are in good agreement with the minimum velocity for the separation of the binary collisional and the dielectric curves in Fig. 3.

The difference between the dielectric and binary collisional curves in this figure lets us appreciate the importance of the plasmon excitation contribution to the total probabilities per unit length. For projectile electron excitation $1s \rightarrow 2p$ this contribution is important at very high velocities ($v/Z_P \geqslant 4$), being about 65% for H^0 projectiles, 26% for He^+ projectiles, and 15% for Li^{2+}. Instead, for projectile electron excitation $1s \rightarrow 2s$, the plasmon contribution is much less important (28% for H projectiles, 4% for He^+, and negligible for higher projectile charges in the same velocity range). Similar results are obtained for electron loss.

The second observation is that Fig. 3 shows the above-mentioned suppression of the excitation inside the solid, i.e., the ratio of in-solid to out-solid probabilities is $R<1$. This effect is very important for H projectiles, with the probabilities per unit length for projectile electron excitation $1s \rightarrow 2p(1s \rightarrow 2s)$ being only 10% (32%) of those corresponding to excitation of H by single-electron impact. For projectile electron loss processes in H-FEG collisions at $v \geqslant 5$ a.u., the probabilities are less than 50% of those of H-e collisions. The suppression is not so drastic for greater nuclear charges, as observed in Fig. 3. This behavior is due to the $\Delta\varepsilon/v$ dependence indicated in Sec. II D, and also explains the tendency to decrease with increasing velocity of the curves in Fig. 3.

B. Energy spectrum

The energy spectrum given by Eq. (14) is calculated for excitation and electron loss of He^+ projectiles due to the collisions with the aluminum FEG at $v=6$ a.u. This velocity is chosen to be high enough for the first Born approximation to give a good estimation of the probabilities and for the plasmon contribution to be appreciable (see Fig. 3). On the other hand, it is low enough to be within the experimental range of possibilities.

In Fig. 4 we plot the dielectric and collisional probabilities as a function of the energy gained by the FEG, $P_{DF}(\omega)$ and $P_{BC}(\omega)$. Also plotted is the subtraction of both of them in order to isolate the plasmon excitation contribution, $P_p(\omega)=P_{DF}(\omega)-P_{BC}(\omega)$. Four cases are displayed in this figure: projectile electron excitations $1s \rightarrow 2s$ and $1s \rightarrow 2p$, de-excitation $2p \rightarrow 1s$, and electron loss from the ground state $1s \rightarrow k$. The de-excitation $2s \rightarrow 1s$ has also been performed giving an energy spectrum similar to the excitation case $1s \rightarrow 2s$.

In the four processes presented in Fig. 4, the plasmon peak appears in the range of energies where the collective mode is possible, i.e., $\omega_p \leqslant \omega \leqslant \omega_p(q_c)$, with $\omega_p(q_c) \simeq 0.75$ a.u. for aluminum [5,38]. The highest peak corresponds to the de-excitation $2p \rightarrow 1s$, but the total probability integrated over the energy absorbed by the FEG is bigger for electron loss than for the transitions to bound states (a factor of 2 with respect to $2p \rightarrow 1s$). The peak obtained for the de-excitation $2p \rightarrow 1s$ is due to the collective modes of excitation of the FEG accompanying this transition, while the biggest total probability for electron loss is due to the binary collisions with the single electrons of the FEG.

In comparing the excitation $1s \rightarrow 2p$ with the de-excitation $2p \rightarrow 1s$, we can see that although the plasmon contribution P_p is bigger in the latter, the binary collisional probability P_{BC} is the same for both transitions, as is expected from detailed balancing.

IV. CONCLUSIONS

Excitation and ionization of hydrogenic projectiles in collision with the free-electron gas (FEG) have been analyzed in the high but non-relativistic energy regime. Probabilities per unit length and energy spectrum have been calculated in the first Born approximation for different hydrogenic projectiles such as H^0, He^+, Li^{2+}, and B^{4+} colliding with aluminum FEG. The response of the medium to the external perturbation has been described by employing the Mermin-Lindhard dielectric function.

Projectile excitation probabilities per unit length are found to be smaller than those corresponding to the collisions with an equivalent density of single electrons. This suppression of the excitation in in-solid collisions is maximum for H projectiles, and diminishes for higher nuclear charges. We explain this behavior in terms of the collective effect (shielding) of the FEG. The difference between in-solid and out-solid probabilities of projectile excitation becomes greater when the minimum momentum transferred to the FEG diminishes (either by increasing the impact velocity v or decreasing the energy transferred to the atomic electron $\Delta\varepsilon$). Although less important, this shielding should also be found in the excitation of target inner shells if the local plasma approximation is used [39].

By comparing probabilities per unit length obtained using a binary collisional formalism and those using the dielectric formalism, we evaluate the importance of the plasmon excitation for different impact velocities. We find this contribution to be more important for projectile-electron-allowed transitions $1s \leftrightarrow 2p$ than for forbidden ones $1s \leftrightarrow 2s$, or projectile electron loss, where it is appreciable only at very high velocities. An estimation of the threshold velocity for plasmon excitation is found to be in good agreement with the present theoretical results.

The relative importance of the FEG in the projectile excitation processes is estimated by comparing our results with the theoretical cross sections corresponding to the interaction with the whole target atom. For He^+ projectiles the excitation and loss probabilities due to the interaction with the FEG represents about 30% of the total probabilities considering the whole target atoms. These values are expected to be more important in the case of H^0 projectiles.

ACKNOWLEDGMENT

We acknowledge P. Echenique for suggesting the investigation of this subject.

[1] J. Lindhard, K. Dan. Vidensk. Selsk. Mat. Fys. Medd. **28**, 8 (1954).
[2] R. H. Ritchie, Phys. Rev. **114**, 644 (1959).
[3] J. Lindhard and A. Winther, K. Dan. Vidensk. Selsk. Mat. Fys. Medd. **34**, 4 (1964).
[4] P. Nozière, *Theory of Interaction Fermi Systems* (Benjamin, New York, 1964).
[5] D. Pines, *Elementary Excitations in Solids* (Benjamin, New York, 1964).
[6] A. L. Fetter and J. D. Walecka, *Quantum Theory of Many Particle Systems* (McGraw-Hill, New York, 1971).
[7] P. M. Echenique, F. Flores, and R. H. Ritchie, Solid State Phys. **43**, 229 (1990), and references therein.
[8] I. Abril, R. Garcia-Molina, C. D. Denton, F. J. Pérez-Pérez, and N. R. Arista, Phys. Rev. A **58**, 357 (1998).
[9] T. Kaneko, Phys. Rev. A **33**, 1602 (1986).
[10] D. G. Arbó and J. E. Miraglia, Phys. Rev. A **58**, 2970 (1998).
[11] Y. Haruyama, Y. Kanamori, T. Kido, and F. Fukuzawa, J. Phys. B **15**, 779 (1982).
[12] Y. Haruyama, Y. Kanamori, T. Kido, A. Itoh, and F. Fukuzawa, J. Phys. B **16**, 1225 (1983).
[13] J.-P. Rozet, A. Chetioui, P. Piquemal, D. Vernhet, K. Wohrer, C. Stephan, and L. Tassan-Got, J. Phys. B **22**, 33 (1989).
[14] C. C. Montanari, M. S. Gravielle, V. D. Rodriguez, and J. E. Miraglia, Phys. Rev. A **61**, 022901 (2000).
[15] P. Nicolaï, M. Chabot, J.-P. Rozet, M. F. Politis, A. Chetioui, C. Stephan, A. Touati, D. Vernhet, and K. Wohrer, J. Phys. B **23**, 3609 (1990).
[16] D. Vernhet, J.-P. Rozet, I. Bailly-Despiney, C. Stephan, A. Cassimi, J.-P. Grandin, and L. J. Dubé, J. Phys. B **31**, 117 (1998).
[17] J.-P. Rozet, D. Vernhet, I. Bailly-Despiney, C. Fourment, and L. J. Dubé, J. Phys. B **32**, 4677 (1999).
[18] M. Rösler and F. J. Garcia de Abajo, Phys. Rev. B **54**, 17 158 (1996).
[19] C. O. Reinhold and J. Burgdörfer, Phys. Rev. A **55**, 450 (1997).
[20] M. R. C. McDowell and J. P. Coleman, *Introduction to the Theory of Ion-Atom Collisions* (North-Holland, Amsterdam, 1970).
[21] C. J. Joachain, *Quantum Collision Theory* (North-Holland, Amsterdam, 1975), Vol. 1.
[22] N. D. Mermin, Phys. Rev. B **1**, 2362 (1970).
[23] D. Vrinceanu and M. R. Flannery, Phys. Rev. A **60**, 1053 (1999).
[24] A. Salin, J. Phys. B **22**, 3901 (1989).
[25] F. Salvat, J. M. Fernandez-Varea, and W. Williamson Jr., Comput. Phys. Commun. **90**, 51 (1995).
[26] F. J. Rogers, H. C. Graboske, and D. J. Harwood, Phys. Rev. A **1**, 1577 (1970).
[27] J. Müller and J. Burgdörfer, Phys. Rev. A **43**, 6027 (1991).
[28] A. J. Glick and R. A. Ferrell, Ann. Phys. (N.Y.) **11**, 359 (1960).
[29] K. Tinschert, A. Müller, G. Hofmann, K. Huber, R. Becker, D. C. Gregory, and E. Salzborn, J. Phys. B **22**, 531 (1989).
[30] W. E. Kauppila, W. R. Ott, and W. L. Fite, Phys. Rev. A **1**, 1099 (1970).
[31] M. B. Shah, D. S. Elliott, and H. B. Gilbody, J. Phys. B **20**, 3501 (1987).
[32] B. Peart, D. S. Walton, and K. T. Dolder, J. Phys. B **2**, 1347 (1969).
[33] R. L. Long, D. M. Cox, and S. J. Smith, J. Res. Natl. Bur. Stand., Sect. A **72**, 521 (1968).
[34] W. R. Ott, W. E. Kauppila, and W. L. Fite, Phys. Rev. A **1**, 1089 (1970).
[35] W. L. van Wyngaarden and H. R. J. Walters, J. Phys. B **19**, 929 (1986).
[36] J. Lower, I. E. McCarthy, and E. Weigold, J. Phys. B **20**, 4571 (1987).
[37] T. Kaneko, Phys. Rev. A **32**, 2175 (1985).
[38] D. Isaacson, New York University Report *Radiation and Solid State Laboratory*, 1975 (unpublished).
[39] J. D. Fuhr, V. H. Ponce, F. J. Garcia de Abajo, and P. M. Echenique, Phys. Rev. B **57**, 9329 (1998).